Energy Transfer

DOI: 10.1002/ange.201205082

Perfluorinated Aromatic Spacers for Sensitizing Europium(III) Centers in Dinuclear Oligomers: Better than the Best by Chemical Design?**

Jean-François Lemonnier, Lucille Babel, Laure Guénée, Prasun Mukherjee, David H. Waldeck, Svetlana V. Eliseeva, Stéphane Petoud,* and Claude Piguet**

The unique optical characteristics of lanthanide ions (Ln^{III}) have driven their use in a wide range of applications; however, the efficiency of populating their electronic states directly is limited, and thus there is a great need to create an antenna to capture energy and generate excited Ln^{III} ions. In this context, metal–organic frameworks, hybrid materials, and nanoparticles randomly doped with homo- or heterometallic mixtures of luminescent lanthanide cations (Ln^{III}) are intensively being investigated for engineering luminescent devices for bright-white lighting, for upconversion, and as sensing agents.[1] Although the exact location of the various metals in the final material is crucial for dual ligand-centered/metal-centered emission,[1l,m] for upconversion,[1g] and for directional light-conversion[2a] processes, the preparation of organized polymetallic 4f-4f oligomers and polymers remains rare and challenging.[2] A statistical mechanics (Ising model) analysis suggests that standard repulsive nearest neighbor intermetallic interactions operating in linear polymers with regularly spaced binding sites should provide the targeted ordered …-Ln^1-Ln^2-Ln^1-Ln^2-… microstates.[3,4] Pioneering work in this field has relied on the bulk electropolymerization of didentate 1,10-phenanthroline with thienyl spacers,[5] and the acyclic diene metathesis of tridentate 2,6-bis(benzimidazol-2-yl)pyridine,[6] followed by reaction with [Eu(β-diketonate)$_3$] or Eu(NO$_3$)$_3$ to yield red-emitting metallopolymers. A reliable exploitation of this concept for the development of luminescent materials, however, requires the efficient sensitization of the luminophore through the rational optimization of each photophysical step by using chemical tools.

As a first step toward this goal, the rigid segmental ligand strands **L1**–**L3**, made of two tridentate binding units separated by a rigid and electronically tunable aromatic spacer, have been treated with trivalent europium to give the dinuclear complexes [Eu$_2$(**L**)(hfac)$_6$] (Scheme 1; hfac = hexafluoroacetonato).[7] The use of a simple method for deciphering the various contributions to the sensitization mechanism clearly showed that [Eu$_2$(**L3**)(hfac)$_6$] had the largest global emission quantum yield [$\Phi^{L}_{Eu} = 0.206(7)$, Eqs. (1) and (2)] because of an efficient **L3**→Eu energy transfer step [$\eta^{L\to Eu}_{en.tr.} = 0.47(14)$; Eq. (3), see the dark gray bars in Figure 1].[7]

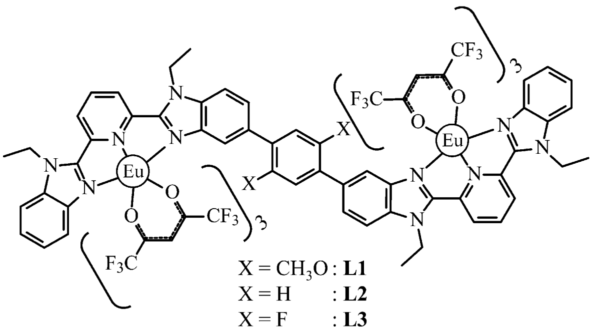

Scheme 1. Chemical structures of complexes [Eu$_2$(**L**)(hfac)$_6$].

$$\Phi^{L}_{Eu} = \eta_{ISC}\,\eta^{L\to Eu}_{en.tr.}\,\Phi^{Eu}_{Eu} \tag{1}$$

$$\eta_{ISC} = \frac{k_{ISC}}{k^{F}_{r} + k^{F}_{nr} + k_{ISC}} \tag{2}$$

$$\eta^{L\to Eu}_{en.tr.} = \frac{2k^{Eu}_{en.tr.}}{k^{P}_{r} + k^{P}_{nr} + k^{Eu}_{en.tr.}} = 2k^{Eu}_{en.tr.}\,\tau^{Eu}_{L}(^{3}\pi^{*}) \tag{3}$$

Theoretical considerations suggest that $\eta^{L\to Eu}_{en.tr.}$ could benefit from a shift of the **L**($^3\pi^*$) state to higher energy through perfluorination of the central aromatic spacer to give **L4** (Scheme 2).[8] Correspondingly, the expected decrease in the k^{F}_{nr} and k^{Eu}_{nr} values, and of the so-called π-conjugation length A_π [Eq. (5)][9] in [Eu$_2$(**L4**)(hfac)$_6$],[7] should optimize both the intersystem crossing efficiency [η_{ISC} =0.6(1), Eq. (2)] and the intrinsic Eu-centered quantum yield [Φ^{Eu}_{Eu} =0.76(2), Eq. (4)] of those previously measured for [Eu$_2$(**L3**)(hfac)$_6$] (dark gray bars in Figure 1).

---

[*] Dr. J.-F. Lemonnier, L. Babel, Prof. Dr. C. Piguet
Department of Inorganic Analytical Chemistry
University of Geneva
30 quai E. Ansermet, CH-1211 Geneva 4 (Switzerland)
E-mail: claude.piguet@unige.ch

Dr. L. Guénée
Laboratory of Crystallography, University of Geneva
24 quai E. Ansermet, CH-1211 Geneva 4 (Switzerland)

Dr. P. Mukherjee, Prof. Dr. D. H. Waldeck
Department of Chemistry, University of Pittsburgh
219 Parkman Avenue, Pittsburgh, PA 15260 (USA)
E-mail: dave@pitt.edu

Dr. S. V. Eliseeva, Prof. Dr. S. Petoud
Centre de Biophysique Moléculaire
CNRS UPR 4301, Rue Charles Sadron
F-45071 Orléans Cedex 2 (France)
E-mail: stephane.petoud@cnrs-orleans.fr

[**] This work was supported through grants from the Swiss National Science Foundation, the National Institutes of Health (through NIH grant R21-EB008257-01A1), the National Science Foundation (CHE-0718755), as well as la Ligue contre le Cancer and the Institut National de la Santé et de la Recherche Médicale (INSERM). The work was carried out within the COST Actions D38 and CM1006.

Supporting information for this article is available on the WWW under http://dx.doi.org/10.1002/anie.201205082.

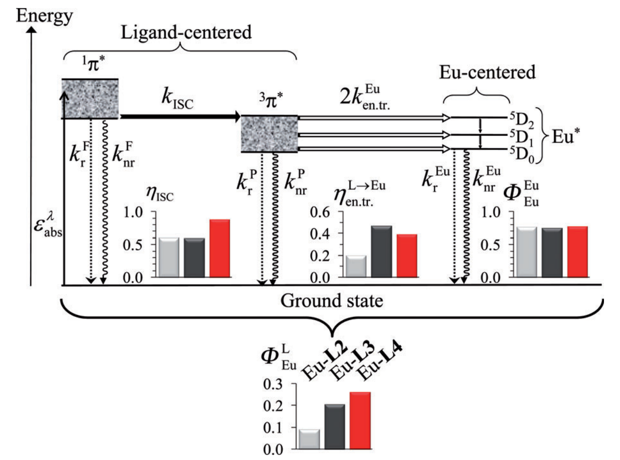

Figure 1. Simplified Jablonski diagram for $[Eu_2(L)(hfac)_6]$ (**L** = **L2**–**L4**) showing the ligand-centered triplet-mediated sensitization mechanism of the two Eu^{3+} ions.[10] The photophysical processes are described by the rate constants: k_r^F for the ligand fluorescence, k_{nr}^F for the internal nonradiative conversion of the ligand, k_r^P for the ligand phosphorescence, k_{nr}^P for nonradiative relaxation from the ligand triplet state, k_r^{Eu} for the emission of Eu*, k_{nr}^{Eu} for the nonradiative decay of Eu*, k_{ISC} for ligand intersystem crossing, and $k^{Eu}_{en.tr.}$ for the ligand-to-metal energy transfer. The efficiencies of intersystem crossing (η_{ISC}), energy transfer ($\eta^{L\rightarrow Eu}_{en.tr.}$), intrinsic quantum yield (Φ^{Eu}_{Eu}), and quantum yield (Φ^{L}_{Eu}) for the global ligand-mediated sensitization of Eu^{III} in $[Eu_2(L)(hfac)_6]$ (solid-state, 293 K) are also shown.

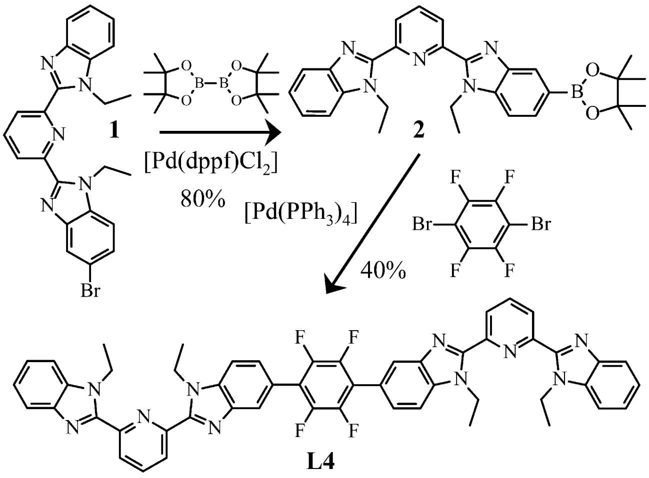

Scheme 2. Synthesis of the perfluorinated ligand **L4**.

$$\Phi^{Eu}_{Eu} = \frac{k_r^{Eu}}{k_r^{Eu} + k_{nr}^{Eu}} = k_r^{Eu} \cdot \tau_{Eu} \qquad (4)$$

$$k_r^F = k_{nr}^F \cdot e^{A_\pi} \qquad (5)$$

The centrosymmetrical perfluorinated ligand **L4** is obtained through two successive palladium-catalyzed Suzuki–Myaura cross-coupling reactions (Scheme 2; see also Figures S1 and S2 in the Supporting Information). Mixing stoichiometric amounts of **L4** with $[Ln(hfac)_3(diglyme)]$ (2.0 equiv) in chloroform gives $[Ln_2(\mathbf{L4})(hfac)_6]$ (Ln = Gd, Eu) in 80 % yield. Slow evaporation of concentrated acetonitrile/chloroform solutions containing the europium complex, provided X-ray quality prisms (see Table S1 in the Supporting Information) including S-shaped centrosymmetrical neutral $[Eu_2(\mathbf{L4})(hfac)_6]$ complexes, in which the Eu atoms are separated by 14.667(1) Å (Figure 2). Each metal center is nine-coordinate in a highly distorted monocapped square antiprismatic polyhedron, produced by the three nitrogen atoms of the bound tridentate aromatic unit and by the six oxygen atoms of the three didentate hexafluoroacetylacetonate moieties, with N1 occupying the capping position (see the Supporting Information). All the bond distances and bond angles are standard (see Tables S2–S4 in the Supporting Information) and the solid-state molecular structures of $[Yb_2(\mathbf{L3})(hfac)_6]$ and $[Eu_2(\mathbf{L4})(hfac)_6]$ are almost superimposable, except for the interannular phenyl–benzimidazole twist angle, which increases from 54.1(1)° to 66.2(1)° (see Figure S3 and Table S5 in the Supporting Information).

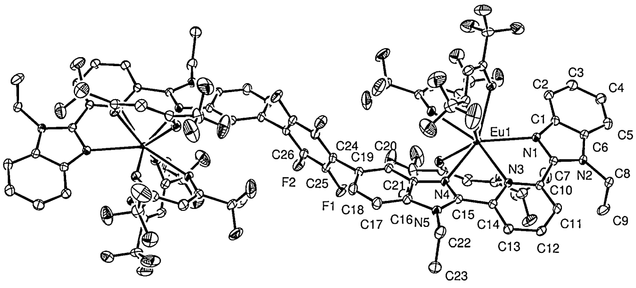

Figure 2. Perspective view of the molecular structure and numbering scheme of $[Eu_2(\mathbf{L4})(hfac)_6]$, as obtained from X-ray diffraction. Thermal ellipsoids are represented at the 30 % probability level and hydrogen atoms are omitted for clarity.

Irradiation into the allowed ligand-centered $^1\pi^* \leftarrow {}^1\pi$ transition of $[Eu_2(\mathbf{L4})(hfac)_6]$ at $\tilde{\nu}_{exc} = 28170\ cm^{-1}$ produces an intense long-lived red emission signal arising from $\mathbf{L4} \rightarrow Eu^{III}$ energy transfer followed by an $Eu(^5D_1)$- and $Eu(^5D_0)$-centered luminescence (see Figure S4 in the Supporting Information). The emission spectrum is dominated by the hypersensitive forced electric dipolar $Eu(^5D_0 \rightarrow {}^7F_2)$ transition centered at $16340\ cm^{-1}$, which leads to the largest global absolute quantum yields in this series ($\Phi^L_{Eu} = 0.26(1)$, solid state, 293 K; Table 1, entry 6).[11] Using Einstein's result for the spontaneous radiative emission rate,[12] the radiative rate constant k_r^{Eu} Table 1, entry 2) is deduced from the I_{tot}/I_{MD} ratio, where I_{tot} is the integrated emission for the $Eu(^5D_0)$ level ($^5D_0 \rightarrow {}^7F_J$, $J = 0$–4) and I_{MD} is the integrated intensity of the magnetic dipolar $Eu(^5D_0 \rightarrow {}^7F_1)$ transition (Table 1, entry 1). In combination with the characteristic lifetime $\tau_{Eu} = 0.90(1)$ ms (Table 1, entry 3), we calculate $\Phi^{Eu}_{Eu} = 0.77(1)$ for the intrinsic Eu-centered quantum yield [Eq. (4); Table 1, entry 4], a value identical to that obtained for $[Eu_2(\mathbf{L3})(hfac)_6]$. This finding implies that the gain in global quantum yields can be assigned specifically to the improved sensitization process $\eta_{sens} = \eta_{ISC}\eta^{L\rightarrow Eu}_{en.tr.} = \Phi^L_{Eu}/\Phi^{Eu}_{Eu} = 0.34(1)$ operating in $[Eu_2(\mathbf{L4})(hfac)_6]$ [Eq. (1); Table 1, entry 7). Given that the experimental ligand-centered fluorescence lifetimes measured for the $[Gd_2(\mathbf{L})(hfac)_6]$ complexes (**L** = **L1**–**L4**, Table S6) are only

Table 1: Experimental global $\left(\Phi_{\mathrm{Eu}}^{\mathrm{L}}\right)$ and intrinsic $\left(\Phi_{\mathrm{Eu}}^{\mathrm{Eu}}\right)$ quantum yields, luminescence lifetimes (τ_{Eu}) as well as calculated energy migration efficiencies (η_{ISC}, $\eta_{\mathrm{en.tr.}}^{\mathrm{L}\rightarrow\mathrm{Eu}}$) and rate constants ($k_{\mathrm{r}}^{\mathrm{Eu}}$, $k_{\mathrm{nr}}^{\mathrm{Eu}}$, $k_{\mathrm{en.tr.}}^{\mathrm{Eu}}$, $k_{\mathrm{r}}^{\mathrm{P}}$, $k_{\mathrm{nr}}^{\mathrm{P}}$, k_{ISC}) for [Eu$_2$(**L**)(hfac)$_6$] in the solid state at 293 K ($k=2$–4).[10]

Compound	[Eu$_2$(**L2**)(hfac)$_6$]	[Eu$_2$(**L3**)(hfac)$_6$]	[Eu$_2$(**L4**)(hfac)$_6$]
Eu-centered luminescence			
$I_{\mathrm{tot}}/I_{\mathrm{MD}}$	17.5(3)	18.2(3)	17.2(2)
$I_{\mathrm{tot}}/I_{\mathrm{MD}}$ [ms^{-1}]	0.86(2)	0.90(2)	0.85(1)
$k_{\mathrm{r}}^{\mathrm{Eu}}$ [ms]	0.88(4)	0.83(15)	0.90(1)
$\Phi_{\mathrm{Eu}}^{\mathrm{Eu}}$	0.76(4)	0.75(1)	0.77(1)
$k_{\mathrm{nr}}^{\mathrm{Eu}}$ [ms^{-1}]	0.21(1)	0.23(4)	0.200(4)
global quantum yield and sensitization efficiency			
$\Phi_{\mathrm{Eu}}^{\mathrm{L}}$	0.092(3)	0.206(7)	0.26(1)
$\eta_{\mathrm{ISC}}\eta_{\mathrm{en.tr.}}^{\mathrm{L}\rightarrow\mathrm{Eu}}$	0.122(7)	0.28(5)	0.34(1)
energy migration and associated rate constants			
$k_{\mathrm{ISC}}^{\mathrm{Gd-\mathbf{L}}}$ [ns^{-1}]	10.0(6)	9(2)	30(4)
$k_{\mathrm{r}}^{\mathrm{F}}+k_{\mathrm{nr}}^{\mathrm{F}}$ [ns^{-1}]	6.71(5)	6.25(3)	4.00(5)
η_{ISC}	0.60(3)	0.59(12)	0.88(15)
$\eta_{\mathrm{en.tr.}}^{\mathrm{L}\rightarrow\mathrm{Eu}}$	0.20(2)	0.47(14)	0.39(6)
$2k_{\mathrm{en.tr.}}^{\mathrm{Eu}}$ [ms^{-1}]	2.1(3)	5.5(2.3)	5.7(2.1)
$k_{\mathrm{r}}^{\mathrm{P}}+k_{\mathrm{nr}}^{\mathrm{P}}$ [ms^{-1}]	8.1(5)	6.3(8)	9.1(2.5)
reference	[7]	[7]	this work

30–60 ps, one can assume that the energy migration processes in [Eu$_2$(**L**)(hfac)$_6$] are described well by the exclusive contribution of the triplet state, as shown in Figure 1.[7,13] Considering that 1) the sum of the radiative and internal nonradiative conversion rate constants $k_{\mathrm{r}}^{\mathrm{F}}+k_{\mathrm{nr}}^{\mathrm{F}}$ controlling the relaxation of the $^1\pi^*$ excited state in the free ligand are the same in the gadolinium complex [Gd$_2$(**L4**)(hfac)$_6$] and that 2) $k_{\mathrm{ISC}}^{\mathbf{L4}} \ll k_{\mathrm{ISC}}^{\mathrm{Gd-\mathbf{L4}}}$, because of the paramagnetic and heavy atom effects generated by the Gd$^{\mathrm{III}}$ center,[14] the introduction of the experimental characteristic lifetimes of $^1\pi^*$ measured in **L4** ($\tau_{\mathrm{L}}^{\mathbf{L4}}(^1\pi^*)=0.25(2)$ ns) and in [Gd$_2$(**L4**)(hfac)$_6$] [$\tau_{\mathrm{L}}^{\mathrm{Gd-\mathbf{L4}}}(^1\pi^*)=0.029(6)$ ns; see also Table S6 in the Supporting Information) into Equation (6) gives $k_{\mathrm{ISC}}^{\mathrm{Gd-\mathbf{L4}}}=30(4)$ ns^{-1}

$$\begin{aligned}\frac{1}{\tau_{\mathrm{L}}^{\mathrm{Gd-\mathbf{L}}}(^1\pi^*)}-\frac{1}{\tau_{\mathrm{L}}^{\mathbf{L}}(^1\pi^*)} &= \left(k_{\mathrm{r}}^{\mathrm{F}}+k_{\mathrm{nr}}^{\mathrm{F}}+k_{\mathrm{ISC}}^{\mathrm{Gd-\mathbf{L}}}\right)-\left(k_{\mathrm{r}}^{\mathrm{F}}+k_{\mathrm{nr}}^{\mathrm{F}}+k_{\mathrm{ISC}}^{\mathbf{L}}\right)\\ &= k_{\mathrm{ISC}}^{\mathbf{L}}-k_{\mathrm{ISC}}^{\mathrm{Gd-\mathbf{L}}} \approx k_{\mathrm{ISC}}^{\mathrm{Gd-\mathbf{L}}}\end{aligned} \tag{6}$$

(Table 1, entry 8) and $k_{\mathrm{r}}^{\mathrm{F}}+k_{\mathrm{nr}}^{\mathrm{F}}=4.00(5)$ ns^{-1} (Table 1, entry 9), from which $\eta_{\mathrm{ISC}}=0.88(15)$ can be deduced with Equation (2) (Table 1, entry 10).[7]

Finally, the energy transfer efficiency $\eta_{\mathrm{en.tr.}}^{\mathrm{L}\rightarrow\mathrm{Eu}}=\eta_{\mathrm{sens}}/\eta_{\mathrm{ISC}}=0.39(6)$ and the associated rate constant $2k_{\mathrm{en.tr.}}^{\mathrm{Eu}}=\left[\eta_{\mathrm{en.tr.}}^{\mathrm{L}\rightarrow\mathrm{Eu}}/\left(1-\eta_{\mathrm{en.tr.}}^{\mathrm{L}\rightarrow\mathrm{Eu}}\right)\right]\left(k_{\mathrm{r}}^{\mathrm{P}}+k_{\mathrm{nr}}^{\mathrm{P}}\right)=5.7(2.1)$ ms^{-1} [Eq. (3), with $\left(k_{\mathrm{r}}^{\mathrm{P}}+k_{\mathrm{nr}}^{\mathrm{P}}\right)=1/\tau_{\mathrm{L}}^{\mathrm{Gd-\mathbf{L4}}}(^3\pi^*)=9.1(2.5)$ ms^{-1}] calculated for [Eu$_2$(**L4**)(hfac)$_6$] (Table 1, entries 11 and 12) indicates no noticeable improvement in these parameters on changing from the difluorinated (**L3**) to the perfluorinated (**L4**) spacer, despite the 500–1000 cm^{-1} blue shift of the ligand-centered $^1\pi^*$ (Figure S5 in the Supporting Information) and $^3\pi^*$ (Figure S6 in the Supporting Information) excited states. Our simple method for dissecting the sensitization mechanism[7] shows that the gain in the global quantum yield $\Phi_{\mathrm{Eu}}^{\mathrm{L}}$ for the complex [Eu$_2$(**L4**)(hfac)$_6$] compared to [Eu$_2$(**L3**)(hfac)$_6$] indeed results from an optimization of the intersystem crossing process η_{ISC} (Figure 1).

Scrutiny of the various rate constants (Table 1 and see Table S7 in the Supporting Information) reveals that the decrease in the radiative and internal conversion rate constants $k_{\mathrm{r}}^{\mathrm{F}}+k_{\mathrm{nr}}^{\mathrm{F}}$ for the ligand-centered **L**($^1\pi^*$) state along the series **L2** > **L3** > **L4** acts to improve η_{ISC} [Eq. (2)], but it is the remarkable increase in $k_{\mathrm{ISC}}^{\mathrm{Ln-\mathbf{L}}}$ of [Ln$_2$(**L4**)(hfac)$_6$] which eventually controls the overall intersystem crossing efficiency.

The physical origin of this beneficial effect can be traced back to the golden-rule expression for radiationless transitions [Eq. (7)]:[15]

$$k_{\mathrm{ISC}}=\frac{2\pi}{\hbar}\left\langle ^1\pi^*|H_{\mathrm{SO}}|^3\pi^*\right\rangle^2 \mathrm{FCWDS} \tag{7}$$

where FCWDS is the Franck–Condon weighted density of states. It accounts for the density of vibrational states in the triplet state and their vibrational overlap with the singlet vibrational state. A model that accounts for the thermal population of levels and uses a single quantum mode of frequency ω is commonly associated with the Marcus–Levich–Jortner theory for electron transfer [Eq. (8)]:[16]

$$\mathrm{FCWDS}=\frac{\exp(-S)}{\sqrt{4\pi RT}}\sum_{n=0}^{\infty}\frac{S^n}{n!}\exp\left[-\frac{(\Delta E+n\hbar\omega+\lambda)}{4\lambda RT}\right] \tag{8}$$

The spin–orbit coupling matrix element $\left\langle ^1\pi^*|H_{\mathrm{SO}}|^3\pi^*\right\rangle$ reaches a maximum for nonplanar polyaromatic molecules containing heavy paramagnetic atoms in the molecular frame;[16,17] two conditions which are fulfilled by all the [Eu$_2$(**L**)(hfac)$_6$] complexes described in this study. We note, however, that the deviation from planarity, as measured by the interplanar phenyl–benzimidazole angles, increases along the series **L2** (25.26(4)°) < **L3** (54.1(1)°) < **L4** (66.2(1)°), in line with the k_{ISC} values [Eq. (7) and Table 1). The Franck–Condon weighted density of states (FCWDS) depends on the singlet–triplet energy splitting $\Delta E=E(^1\pi^*)-E(^3\pi^*)$ and on the reorganization energy λ, which corresponds to the energy difference between the triplet and the singlet state at its equilibrium geometry [Eq. (8)].[18] Within the limitation of parabolic surfaces, this energy parameter, along with the ΔE value, provides the energy gap for $n=0$. The successive fluorination of the ligands along the series [Eu$_2$(**L**)(hfac)$_6$] (**L2**–**L4**) is known to significantly affect the frontier orbitals, and hence the λ as well as ΔE and FCWDS values in Equation (8).[7] While a quantitative understanding of the changes in λ requires sophisticated theoretical calculations of the vibrational coupling scheme controlling the Huang–Rhys factors (S),[15,16] Equations (7) and (8) predict that the increasing ligand-centered energy gap ΔE observed along the series **L2** (3550 cm^{-1}) ≈ **L3** (3230 cm^{-1}) < **L4** (5200 cm^{-1}) should lower the k_{ISC} and η_{ISC} values. The apparent contradiction with our experimental results (Table 1, entries 8 and 10) can be resolved by including higher lying triplet states $^3\pi^*_{n>1}$ in the model, an approach used successfully for oligothiophenes[15] and helicenes.[15b] This counterintuitive correlation was noticed empirically for other polyaromatic chromophores, and it was suggested as a "rule-of-thumb" that a singlet–triplet gap of $E(^1\pi^*)-E(^3\pi^*)\geq 5000$ cm^{-1} warrants inclusion of quantitative intersystem crossing processes in Tb and Eu complexes.[19] Given that the singlet–triplet energy gap can be readily calculated by using DFT[7] or semiempirical[8] methods, computations may be useful for identifying simple chemical and structural modifications that will enhance the quantum efficiency further.

In conclusion, the application of this simple method for analyzing the various contributions to the sensitization of Eu^{III} luminescence shows that perfluorination of the remote phenyl spacer in the rigid single-stranded dumbbell-shaped [Eu$_2$(**L4**)(hfac)$_6$] oligomer optimizes both intersystem crossing efficiency and the intrinsic Eu^{III} quantum yield, thus maximizing the global quantum yields in these polyaromatic rigid complexes (red bars in Figure 1).

Received: June 28, 2012

Keywords: energy conversion · fluorinated ligands · intersystem crossing · lanthanides · ligand effects

---

[1] a) J. Kido, Y. Okamoto, *Chem. Rev.* **2002**, *102*, 2357–2368; b) R. C. Evans, P. Douglas, C. J. Winscom, *Coord. Chem. Rev.* **2006**, *250*, 2093–2126; c) A. de Bettencourt-Dias, *Dalton Trans.* **2007**, 2229–2241; d) K. Binnemans, *Chem. Rev.* **2009**, *109*, 4283–4374; e) N. Kerbellec, D. Kustaryono, V. Haquin, M. Etienne, C. Daiguebonne, O. Guillou, *Inorg. Chem.* **2009**, *48*, 2837–2843; f) G.-L. Law, K.-L. Wong, H.-L. Tam, K.-W. Cheah, W.-T. Wong, *Inorg. Chem.* **2009**, *48*, 10492–10494; g) K. Zheng, D. Zhang, D. Zhao, N. Liu, F. Shi, W. Qin, *Phys. Chem. Chem. Phys.* **2010**, *12*, 7620–7625; h) M. A. Katkova, M. N. Bochkarev, *Dalton Trans.* **2010**, *39*, 6599–6612; i) S. V. Eliseeva, J.-C. G. Bünzli, *Chem. Soc. Rev.* **2010**, *39*, 189–227; j) G. M. Farinola, R. Ragni, *Chem. Soc. Rev.* **2011**, *40*, 3467–3482; k) Y. Cui, Y. Yue, G. Qian, B. Chen, *Chem. Rev.* **2012**, *112*, 1126–1162; l) Y. Liu, M. Pan, Q.-Y. Yang, L. Fu, K. Li, S.-C. Wei, C.-Y. Su, *Chem. Mater.* **2012**, *24*, 1954–1960; m) D. F. Sava, L. E. S. Rohwer, M. A. Rodriguez, T. M. Nenoff, *J. Am. Chem. Soc.* **2012**, *134*, 3983–3986.

[2] a) J.-C. G. Bünzli, C. Piguet, *Chem. Rev.* **2002**, *102*, 1897–1928; b) C. M. G. dos Santos, A. J. Harte, S. J. Quinn, T. Gunnlaugsson, *Coord. Chem. Rev.* **2008**, *252*, 2512–2527; c) S. Swavey, R. Swavey, *Coord. Chem. Rev.* **2009**, *253*, 2627–2638; d) S. Faulkner, L. S. Natrajan, W. S. Perry, D. Sykes, *Dalton Trans.* **2009**, 3890–3899; e) P. A. Vigato, V. Peruzzo, S. Tamburini, *Coord. Chem. Rev.* **2009**, *253*, 1099–1201; f) C. Lincheneau, F. Stomeo, S. Comby, T. Gunnlaugsson, *Aust. J. Chem.* **2011**, *64*, 1315–1326.

[3] a) M. Borkovec, J. Hamacek, C. Piguet, *Dalton Trans.* **2004**, 4096–4105; b) C. Piguet, M. Borkovec, J. Hamacek, K. Zeckert, *Coord. Chem. Rev.* **2005**, *249*, 705–726.

[4] N. Dalla-Favera, J. Hamacek, M. Borkovec, D. Jeannerat, G. Ercolani, C. Piguet, *Inorg. Chem.* **2007**, *46*, 9312–9322.

[5] X.-Y. Chen, X. Yang, B. J. Holliday, *J. Am. Chem. Soc.* **2008**, *130*, 1546–1547.

[6] B. M. McKenzie, R. J. Wojtecki, K. A. Burke, C. Zhang, A. Jakli, P. T. Mather, S. J. Rowan, *Chem. Mater.* **2011**, *23*, 3525–3533.

[7] J.-F. Lemonnier, L. Guénée, C. Beuchat, T. A. Wesolowski, P. Mukherjee, D. H. Waldeck, K. A. Gogik, S. Petoud, C. Piguet, *J. Am. Chem. Soc.* **2011**, *133*, 16219–16234.

[8] R. O. Freire, R. Q. Albuquerque, S. A. Junior, G. B. Rocha, M. E. Mesquita, *Chem. Phys. Lett.* **2005**, *405*, 123–126.

[9] Y. Yamaguchi, Y. Matsubara, T. Ochi, T. Wakamiya, Z.-I. Yoshida, *J. Am. Chem. Soc.* **2008**, *130*, 13867–13869.

[10] For the sake of clarity and conciseness in the discussions, the kinetic data collected for **L1**, which bears electron-donating methoxy groups, are not further considered in Figure 1 and Table 1.

[11] Global quantum yields up to 64% have been reported for polynuclear Eu^{III} complexes, see K. Miyata, T. Ohba, A. Kobayashi, M. Kato, T. Nakanishi, K. Fushimi, Y. Hasegawa, *ChemPlusChem* **2012**, *77*, 277–280.

[12] $k_{\mathrm{r}}^{\mathrm{Eu}} = A(\Psi_J, \Psi_{J'}) = A_{\mathrm{MD},0}\, n^3 (I_{\mathrm{tot}}/I_{\mathrm{MD}})$ with $A_{\mathrm{MD},0} = 14.65\ \mathrm{s}^{-1}$ for the magnetic dipolar Eu($^5\mathrm{D}_0 \rightarrow {}^7\mathrm{F}_1$) transition and a refractive index $n = 1.5$: A. Aebischer, F. Gumy, J.-C. G. Bünzli, *Phys. Chem. Chem. Phys.* **2009**, *11*, 1346–1353 and references therein.

[13] a) N. Sabbatini, M. Guardigli, I. Manet, *Handbook on the Physics and Chemistry of Rare Earths*, *Vol. 23* (Eds.: K. A. Gschneidner, Jr., L. Eyring), Elsevier Science, Amsterdam, **1996**, pp. 69–120; b) S. Faulkner, S. J. Pope, B. P. Burton-Pye, *Appl. Spectrosc. Rev.* **2005**, *40*, 1–35; c) M. D. Ward, *Coord. Chem. Rev.* **2010**, *254*, 2634–2642.

[14] a) S. Tobita, M. Arakawa, I. Tanaka, *J. Phys. Chem.* **1984**, *88*, 2697–2702; b) S. Tobita, M. Arakawa, I. Tanaka, *J. Phys. Chem.* **1985**, *89*, 5649–5654.

[15] D. Beljonne, Z. Shuai, G. Pourtois, J. L. Brédas, *J. Phys. Chem. A* **2001**, *105*, 3899–3907, and references therein.

[16] a) J. Jortner, M. Bixon, *Adv. Chem. Phys.* **1999**, *106*, 35–202; b) J. L. Brédas, D. Beljonne, V. Coropceanu, J. Cornil, *Chem. Rev.* **2004**, *104*, 4971–5003; c) K. Schmidt, S. Brovelli, V. Coropceanu, D. Beljonne, J. Cornil, C. Bazzini, T. Caronna, R. Tubino, F. Meinardi, Z. Shuai, J. L. Brédas, *J. Chem. Phys. A* **2007**, *111*, 10490–10499.

[17] A. Monguzzi, R. Tubino, S. Hoseinkhani, M. Campione, F. Meinardi, *Phys. Chem. Chem. Phys.* **2012**, *14*, 4322–4332.

[18] For intersystem crossing, solvent effects are expected to be small and are not considered in the determination of λ. As a first approximation, $\lambda = 1500$–$2000\ \mathrm{cm}^{-1}$ are realistic values for polyaromatic scaffolds.[15,16]

[19] F. J. Steemers, W. Verboom, D. N. Reinhoudt, E. B. van der Tol, J. W. Verhoeven, *J. Am. Chem. Soc.* **1995**, *117*, 9408–9414.